ESTIMATING UNCERTAINTY IN PRESSURE-BASED SOUND POWER MEASUREMENT DUE TO SPATIAL SAMPLING AND NEAR FIELDS

Hannes Pomberger[1], Franz Zotter[1], Robert Höldrich[1], Stephan Brandl[2]

[1]Institute of Electronic Music and Acoustics,
University of Music and Performing Arts, Graz
[2]AVL-List GmbH, Hans-List-Platz 1, 8020 Graz

Abstract: *The engine sound power is a typical benchmark of combustion engines for vehicles, as it delivers a rough over-all estimation of how loud an engine could be when built into a car. The grade 1 procedure for simultaneous sound power measurement considers 20 microphone positions around the engine in an anechoic room, and an engineering (grade 2) procedure typically employs five measurement positions at one meter distance from the engine surface in a semi-anechoic room. In all cases, far-field conditions are considered.*
In this study, we compare uncertainties of typical and spherical-harmonics-based estimation procedures of the sound power using different measurement grid positions. To accomplish this, we take simulated engine data (AVL Excite) as a reliable ground-truth. This allows us to illustrate uncertainties related to the measurement grid and the systematic effect of acoustic near fields at low frequencies. We discuss alternative sampling and computation schemes.

Keywords: sound power, combustion engine, spherical harmonics

1. INTRODUCTION

The norm [1] proposes several grade 1 methods for sound power measurement. In one of them, simultaneous measurements in an anechoic room are specified on a grid of $\mathrm{M} = 20$ (if necessary 40) points on a sphere. The spherical grid is proposed with the idea of providing equal area coverage. Moreover, far field conditions are assumed to be met when the radius R of the measurement grid is at least a fourth wave length, one meter, and twice the largest source diameter. At one frequency, the underlying estimation of sound power then simply relates to

$$\hat{\Pi} = \frac{1}{2}\,\frac{1}{\rho c}\,\frac{4\pi \mathrm{R}^2}{\mathrm{M}} \sum_{i=1}^{\mathrm{M}} |p_i|^2. \tag{1}$$

The norm text displays the equation in a somewhat different look, as values are in dB and several constants, corrections, and normalizations are gathered into simplified expressions.

Essentially, the estimation above derives from the analytic definition of the sound power

$$\Pi = \frac{1}{2} \oint_S \Re\{p\,\boldsymbol{v}^*\} \cdot \mathrm{d}\boldsymbol{S}. \tag{2}$$

In the free field, the particle velocity far away from the source is aligned with the outward normal and related to sound pressure by the free-field impedance $v = \frac{p}{\rho c}$:

$$\Pi = \frac{1}{2}\,\frac{1}{\rho c} \oint_S |p|^2 \,\mathrm{d}S. \tag{3}$$

Eq. (1) is the discretized version of this far-field integral using the average surface element $\frac{4\pi \mathrm{R}^2}{\mathrm{M}}$.

Assuming perfectly calibrated and placed microphones in a perfect measurement room, the alert reader has noticed two sources of estimation uncertainty:

- the far field assumption,
- the spatial discretization of the integral.

Clearly, practical measurement will probably always be accessible only through spatially discrete microphone placement. And some pre-assumptions about sound radiation might always be necessary.

This contribution discusses uncertainties related to different sound power measurement setups using a simulated car engine. The simulation allows us to vary the discretization of

[1]corresponding auhtor pomberger@iem.at

the integral, from the spiral-type sampling proposed in the norm to alternative sampling schemes. Beside the discussion of the effect of sampling, we discuss a strategy to avoid the typical over-estimation of the sound power at low frequencies due to the typical violation of the far field assumption.

2. SIMULATED ENGINE AS TEST OBJECT FOR SOUND POWER

This study uses a simulated engine data obtained from the AVL Excite[3] environment. Sound pressure emitted by the simulated engine can be evaluated on a fine grid as shown in Figure 1. We obtain the wave spectrum $c_{nm}(k)$ of the engine at every wave number $k = \omega/c$, which allows us to evaluate sound pressure at any spherical coordinate r, φ, ϑ

$$p = \sum_{n=0}^{\infty} \sum_{m=-n}^{n} c_{nm}(k)\, h_n(kr)\, Y_n^m(\varphi, \vartheta), \qquad (4)$$

using the spherical Hankel functions $h_n(kr)$ of the second kind, and the spherical harmonics $Y_n^m(\varphi, \vartheta)$.

From the above equation, an accurate ground-truth formulation of the sound power is defined as

$$\begin{aligned} \Pi &= \frac{1}{2} \sum_{n,m} \Re \left\{ \mathrm{R}^2 h_n(k\mathrm{R}) \left[\frac{-\mathrm{i}}{\rho\, c}\, h_n'(k\mathrm{R}) \right]^* \right\} |c_{nm}(k)|^2 \\ &= \frac{1}{2} \frac{1}{\rho\, c} \frac{1}{k^2} \sum_{n,m} |c_{nm}(k)|^2. \end{aligned} \qquad (5)$$

Octave-band averaged sound power levels referenced to 10^{-12} W at different engine speeds are shown in Figure 1.

3. SOUND POWER ESTIMATION USING ISO 3745

Obviously, the orientation of the measurement grid relative to the source does not change the radiated power. However, the estimated sound power might vary for different relative orientations. As the relative orientation is arbitrary, we propose to use this variation to quantify the uncertainty caused by the measurement grid.

Using J uniformly distributed random rotations of a unit sphere, see [4, p. 117], a set of sound power estimations $\{\hat{\Pi}_1, \ldots \hat{\Pi}_j, \ldots \hat{\Pi}_\mathrm{J}\}$ is achieved by applying the random rotations to the measurement grid. The deviation from the ground-truth value in dB is calculated by $\Delta L_{\mathrm{w,j}} = 10 \log_{10}(\Pi) - 10 \log_{10}(\hat{\Pi}_j)$.

ISO 3745 20 point grid

In accordance with the norm, we choose $\mathrm{R} = 1.4\mathrm{m}$ for a lowest frequency of interest of about 60Hz. Using the 20 point grid proposed in the norm, see [1, Table C.1] a set of $\mathrm{J} = 1000$ randomly rotated realization was generated and used for the following statistical analyses, see Figure 2.

[3] http://www.avl.com/web/ast/excite

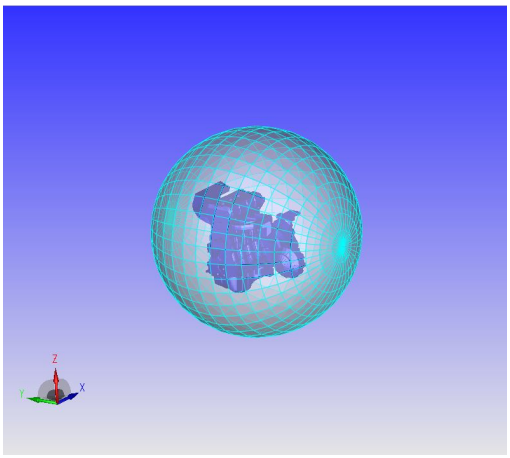

(a) Simulated engine in AVL Excite

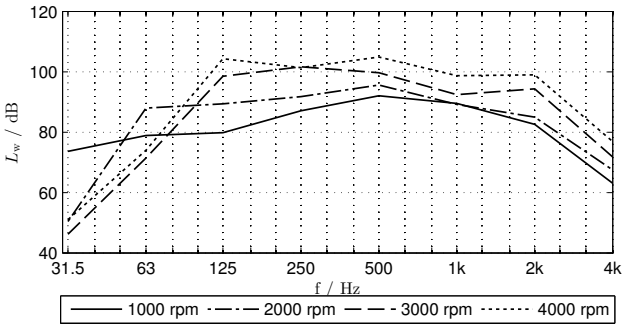

(b) Ground truth octave sound power level

Fig. 1: Engine simulated in AVL Excite.

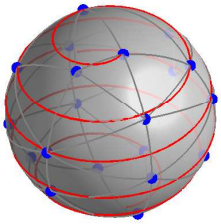

(a) 20 measurement grid from ISO 3745 [1]

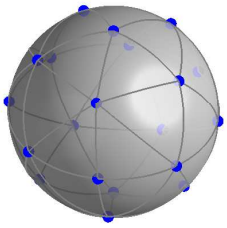

(b) 20 equal area partitioning points [2]

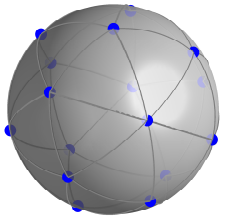

(c) 16 maximum determinant points [3]

Fig. 2: Sampling schemes.

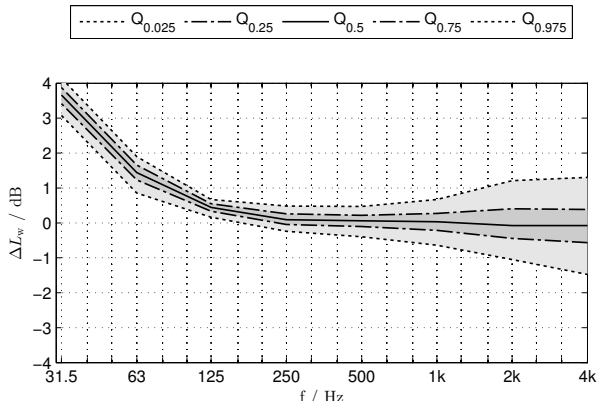

(a) 1000 rpm

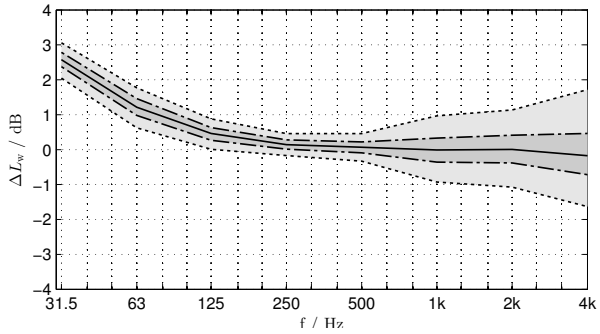

(b) 2000 rpm

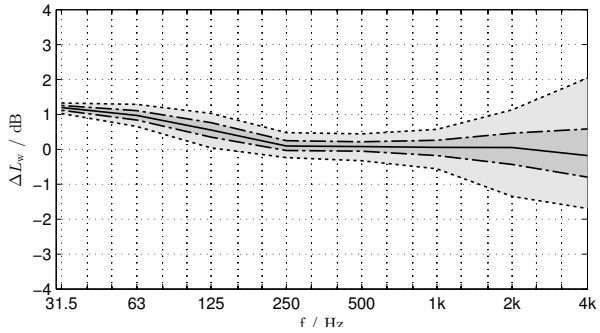

(c) 3000 rpm

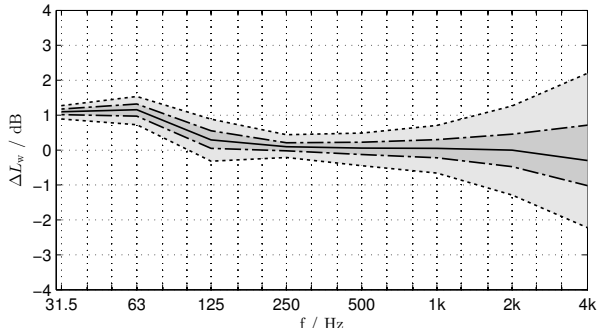

(d) 4000 rpm

Fig. 3: Uncertainty of the ISO 3745 20 point grid, octave band average, (a) 1000 rpm, (b) 2000 rpm, (c) 3000 rpm, (d) 4000 rpm.

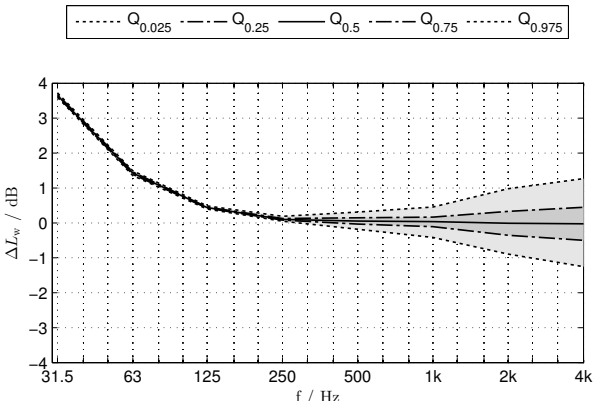

(a) 1000 rpm

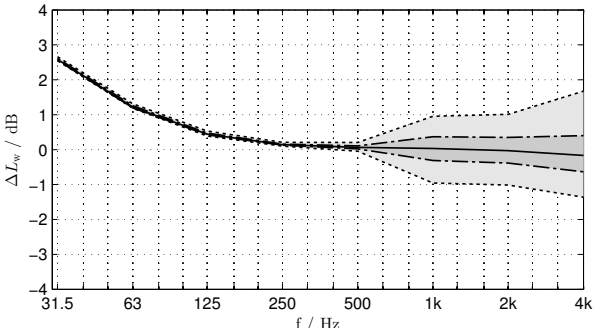

(b) 2000 rpm

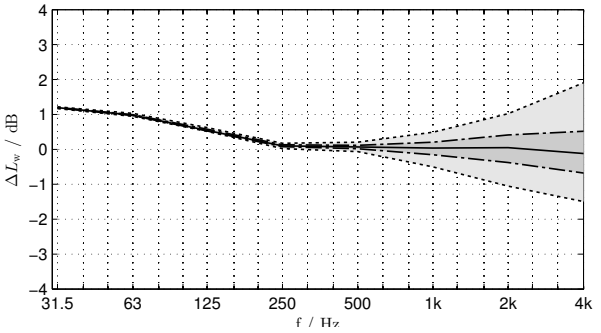

(c) 3000 rpm

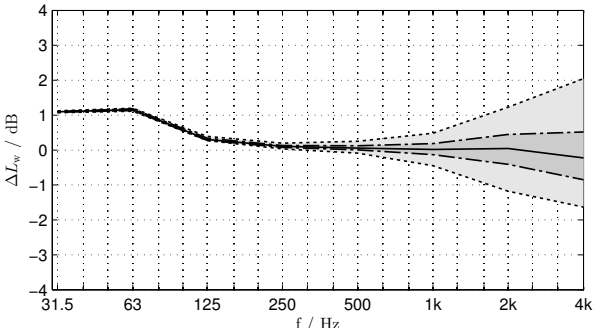

(d) 4000 rpm

Fig. 4: Uncertainty of the equal area partitioning 20 point grid, octave band average, (a) 1000 rpm, (b) 2000 rpm, (c) 3000 rpm, (d) 4000 rpm.

Figure 3 shows an increased statistical spread at high frequencies as the increasingly complex radiation patterns of the engine are not measured densely enough. Less spread is only achieved by denser spatial measurement grids.

At low frequencies, near fields cause a systematic over-estimation of the sound power level. This is because near field components decay more steeply than by $\frac{1}{r}$, which, however is assumed for the far field estimator.

Aside from the systematic error, the decreasing complexity of the engine radiation pattern should yield a vanishing statistical uncertainty at low frequencies. As this is not the case, we could expect that the low-frequency uncertainty is caused by a deficiency of the measurement grid.

4. EQUAL AREA SPHERE PARTITIONING

Assuming a sound source whose low-frequency directivity is of strictly limited complexity, suitable spherical sampling schemes allow to estimate perfectly accurate results [5, 6].

As this is in contrast to results in Figure 3, it is reasonable to test alternative measurement grids that are designed to uniformly cover the sphere. The equal area sphere partitioning scheme [2], cf. Figure. 2, seems to be a good candidate, as it divides the spherical surface into equally large, spherically rectangular areas. Hereby, it might better fulfill the design goal for measurement grids as formulated in [1].

Figure 4 shows less uncertainty using a 20pts equal spherical area partitioning scheme at low frequencies when compared to Fig. 3. Still, there is the systematic over-estimation due to near field components.

5. NEAR-FIELD-INVOLVING ESTIMATOR

If we had a spherical harmonics expanded sound pressure ψ_{nm} at $r = \mathrm{R}$, we would obtain a sound power estimate

$$\Pi = \frac{1}{2}\,\frac{1}{\rho\,c}\,\frac{1}{k^2}\sum_{n,m}\frac{|\psi_{nm}|^2}{|h_n(k\mathrm{R})|^2} \tag{6}$$

through $c_{nm} = \frac{\psi_{nm}}{h_n(k\mathrm{R})}$ that takes near field components into account, which appear for higher than zeroth order.

How to get the pressure expansion coefficient ψ_{nm}?

Using a well-distributed measurement grid, the sound pressure samples $\boldsymbol{p} = [p(\varphi_i, \vartheta_i)]_{i=1\ldots\mathrm{M}}$ can be expanded in the spherical harmonics domain $p = \sum_{n,m}\psi_{nm}Y_n^m(\varphi,\vartheta)$ by the unknown coefficients ψ_{nm}. To find the coefficients, the sampled spherical harmonics up to the orders $0 \le n \le \mathrm{N}$ are written into a matrix $\boldsymbol{Y}_\mathrm{N} = [Y_n^m(\varphi_i,\vartheta_i)]_{i=1\ldots\mathrm{M}}^{n=0\ldots\mathrm{N},|m|\le n}$, as well as the coefficients $\boldsymbol{\psi}_\mathrm{N} = [\psi_{nm}]_{n=0\ldots\mathrm{N},|m|\le n}$. The best fitting $\boldsymbol{p}_\mathrm{N} = \boldsymbol{Y}_\mathrm{N}\,\boldsymbol{\psi}_\mathrm{N}$ estimate is then obtained by

$$\hat{\boldsymbol{\psi}}_\mathrm{N} = \left(\boldsymbol{Y}_\mathrm{N}^\mathrm{T}\boldsymbol{Y}_\mathrm{N}\right)^{-1}\boldsymbol{Y}_\mathrm{N}^\mathrm{T}\,\boldsymbol{p}. \tag{7}$$

To enable inversion, the sampling grid must contain at least $\mathrm{M} \ge (\mathrm{N}+1)^2$ measurement positions that provide a condition number of $\boldsymbol{Y}_\mathrm{N}$, [5]. Inversion is ill-conditioned with the norm grid.

Figure 5 clearly shows that the tendency to over-estimate low-frequency sound power has vanished entirely when using the Eqs. (6)(7). Nevertheless, under-estimation appears to affect the sound power estimate above the 250 Hz octave.

6. MINIMUM DETERMINANT POINTS

The typical summation formula Eq. (1) already yields quite accurate results for the equal area partitioning grid at high frequencies, cf. Figure 4. Consequently, near fields cannot cause under-estimation above the 250 Hz octave in Figure 5. For this reason, the under-estimation can only be caused by the decomposition of the sound pressure into spherical harmonics. Note that the estimation should simplify to Eq. (3) in the far field, because $\lim_{k\mathrm{R}\to\infty}|h_n(k\mathrm{R})|^2 = (k\mathrm{R})^{-2}$

$$\Pi = \frac{1}{2}\,\frac{1}{\rho\,c}\sum_{n,m}\mathrm{R}^2|\psi_{nm}|^2 = \frac{1}{2}\,\frac{1}{\rho\,c}\oint_{\mathbb{S}^2}|p|\,\mathrm{R}^2\mathrm{d}\varphi\,\mathrm{d}\cos\vartheta.$$

The squared sum of $|\psi_{nm}|^2$ and integration over $|p|^2$ is theoretically equal due to Parseval's theorem (unit sphere $\mathbb{S}^2$), $\sum_{nm}|\psi_{nm}|^2 = \oint_{\mathbb{S}^2}|p|^2\,\mathrm{d}\varphi\,\mathrm{d}\cos\vartheta$. Practically, however, we see a difference between far-field estimators with the discretized spherical harmonics transformation and without:

$$\frac{\boldsymbol{p}^\mathrm{H}\,\boldsymbol{Y}_\mathrm{N}\left(\boldsymbol{Y}_\mathrm{N}^\mathrm{T}\boldsymbol{Y}_\mathrm{N}\right)^{-2}\boldsymbol{Y}_\mathrm{N}^\mathrm{T}\,\boldsymbol{p}}{2\rho\,c}\,\mathrm{R}^2 \quad \text{vs.} \quad \frac{\boldsymbol{p}^\mathrm{H}\boldsymbol{p}}{2\rho\,c}\,\frac{4\pi}{\mathrm{M}}\mathrm{R}^2. \tag{8}$$

For a well-distributed grid such as the equal area partitions, non-zero eigenvalues of $\boldsymbol{Y}_\mathrm{N}\left(\boldsymbol{Y}_\mathrm{N}^\mathrm{T}\boldsymbol{Y}_\mathrm{N}\right)^{-2}\boldsymbol{Y}_\mathrm{N}^\mathrm{T}$ would all roughly equal an average unit-sphere surface element $\frac{4\pi}{\mathrm{M}}$.

Whenever the number of sampling points exceeds the number of expansion coefficients $\mathrm{M} > (\mathrm{N}+1)^2$, the $\mathrm{M}\times\mathrm{M}$ matrix gets rank deficient and has only $(\mathrm{N}+1)^2$ non-zero eigenvalues roughly being $\frac{4\pi}{\mathrm{M}}$. Components of the pressure $\boldsymbol{p}$ mapping to the zero eigenvalues will get lost. Such components emerge in the frequency range above 250 Hz, in which the engine radiation pattern gets increasingly complicated.

We conclude that a sampling scheme with $\mathrm{M} = (\mathrm{N}+1)^2$ is favorable to avoid this under-estimation effect. Maximum determinant points [3], cf. Figure 2, allow for well-conditioned spherical harmonics decomposition with $\mathrm{M} = (\mathrm{N}+1)^2$.

Figure 6 shows the estimated sound power level for the $\mathrm{N} = 3$ maximum determinant measurement grid of $\mathrm{M} = 16$ points. Interestingly, the range above 250 Hz has now a slight tendency of over-estimation (less than half a dB). Although maximum determinant points are optimally conditioned, their condition number is normally greater than 1. The decomposition matrix will have a slightly larger norm than $\sqrt{\frac{4\pi}{\mathrm{M}}}$, especially for high order spherical harmonics, which tend to become linearly dependent when sampled.

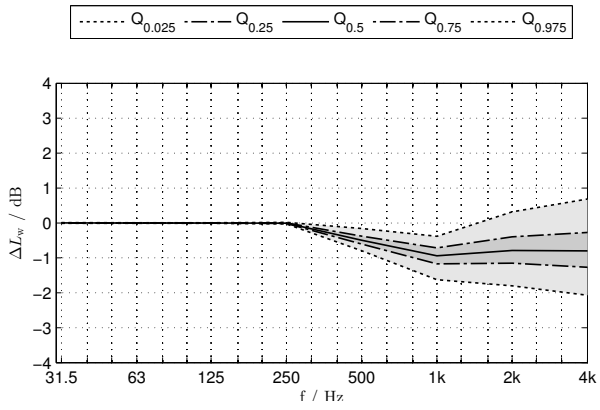

(a) 1000 rpm

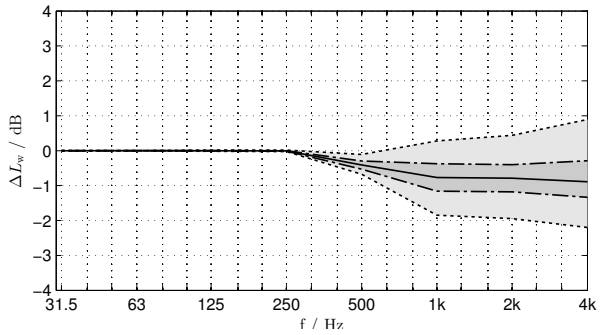

(b) 2000 rpm

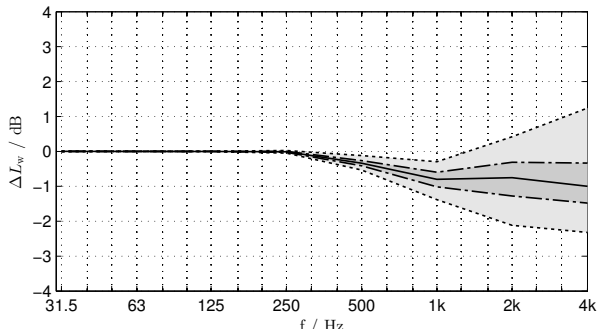

(c) 3000 rpm

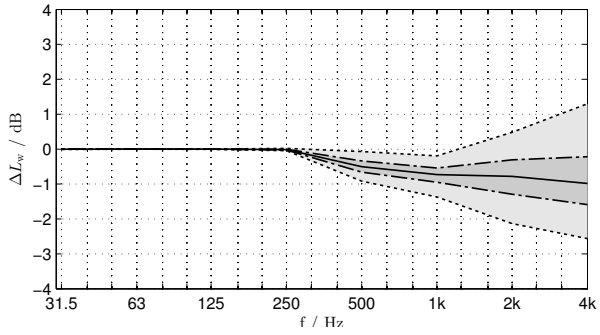

(d) 4000 rpm

Fig. 5: Uncertainty of the equal area partitioning 20 point grid using the near-field-involving estimator, octave band average, (a) 1000 rpm, (b) 2000 rpm, (c) 3000 rpm, (d) 4000 rpm.

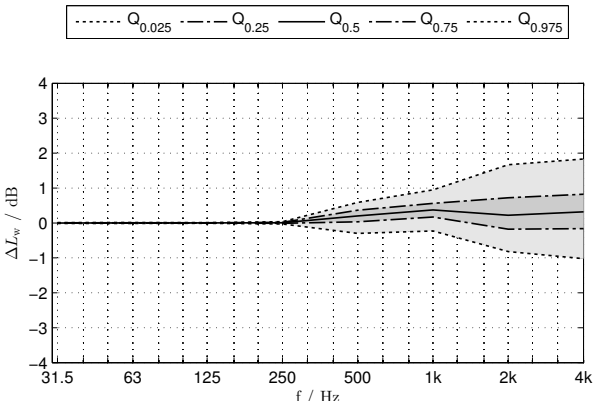

(a) 1000 rpm

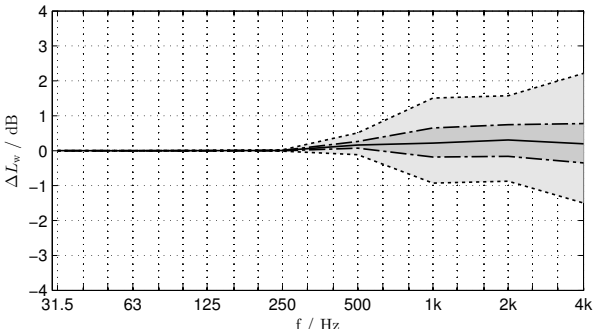

(b) 2000 rpm

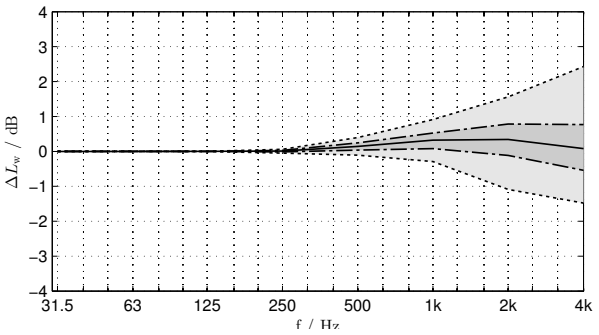

(c) 3000 rpm

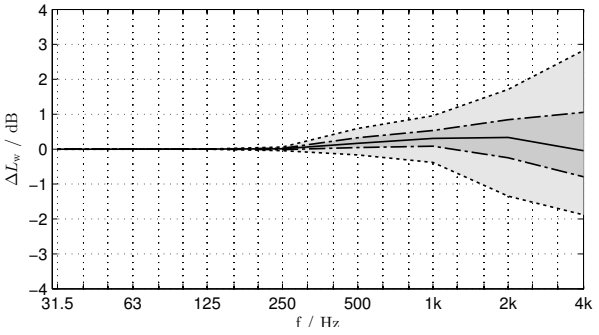

(d) 4000 rpm

Fig. 6: Uncertainty of the md3 16 point grid using the near-field-involving estimator, octave band average, (a) 1000 rpm, (b) 2000 rpm, (c) 3000 rpm, (d) 4000 rpm.

7. COMPOSITE NEAR-FIELD-INVOLVING SOUND POWER ESTIMATOR

The over-estimation tendencies of the squared sound pressure summation Eq. (1) at low frequencies and the slight one of the near-field-involving estimator Eq. (6)(7) at high frequencies yields one conclusion:
It might be best to take the minimum of the far-field and near-field estimators. Hence, we propose a composite estimator

$$\hat{\Pi} = \frac{1}{2\rho\, c}\min\left\{\sum_{n,m}\frac{|\hat{\psi}_{nm}|^2}{k^2|h_n(k\mathrm{R})|^2}, \frac{4\pi\mathrm{R}^2}{\mathrm{M}}\sum_{i=1}^{\mathrm{M}}|p_i|^2\right\}. \quad (9)$$

Figure 7 shows the sound power estimates. The composite estimator is free of noticeable systematic effects in the entire frequency range. The slightly smaller spread around 500 Hz is inherited from the corresponding far-field estimator, which is not depicted.

The estimator is highly accurate until 500 Hz and loses precision in higher bands. As before, more precision in higher bands is only achievable with denser measurement grids.

8. COARSE SAMPLING

As the statistical and systematic deficiencies in highly accurate sound power estimation could be circumvented by suitable decomposition, sampling, and composite estimation, this section discusses estimation with a coarse spatial sampling. To consider near-field-involving sound power estimation up to first-order radiation patterns, a four-points sampling scheme using the corners of a tetrahedron fulfills the requirement $\mathrm{M} = (\mathrm{N}+1)^2$.

Note in the particular case that the spherical harmonics decomposition is done with a perfectly conditioned matrix, so Eq. (6) equals the composite estimator Eq. (9).

Figure 8 shows an increased statistical uncertainty when determining the sound power using these 4 points with the composite near-field-involving estimator. The estimator creates an error of about ± 1 dB up to the 500 Hz octave.

9. CONCLUSION

Sound power measurement procedures are designed for high reproducibility. Standards specify tolerances for acoustic environments, equipment, and also layouts for the microphone positions. Apart from standardized measurement conditions, we showed that orientation differences between the measurement grid and the sound source also cause measurement uncertainty. Sound power estimation with discrete measurement grids exhibits a rotation-variant error, compared to the analytically determined sound power.

We performed a statistical analysis of the rotation-variant error based on a simulated combustion engine in the free

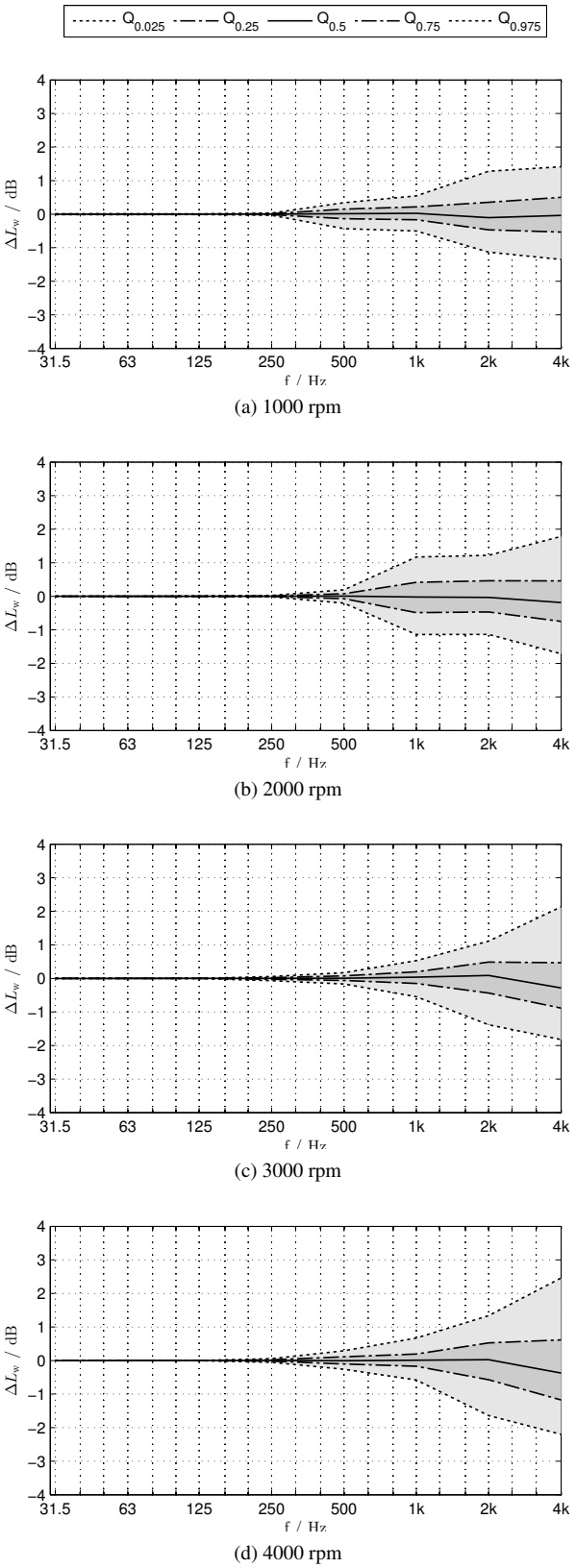

(a) 1000 rpm

(b) 2000 rpm

(c) 3000 rpm

(d) 4000 rpm

Fig. 7: Uncertainty of the md3 16 point grid using the composite near-field-involving estimator, octave band average, (a) 1000 rpm, (b) 2000 rpm, (c) 3000 rpm, (d) 4000 rpm.

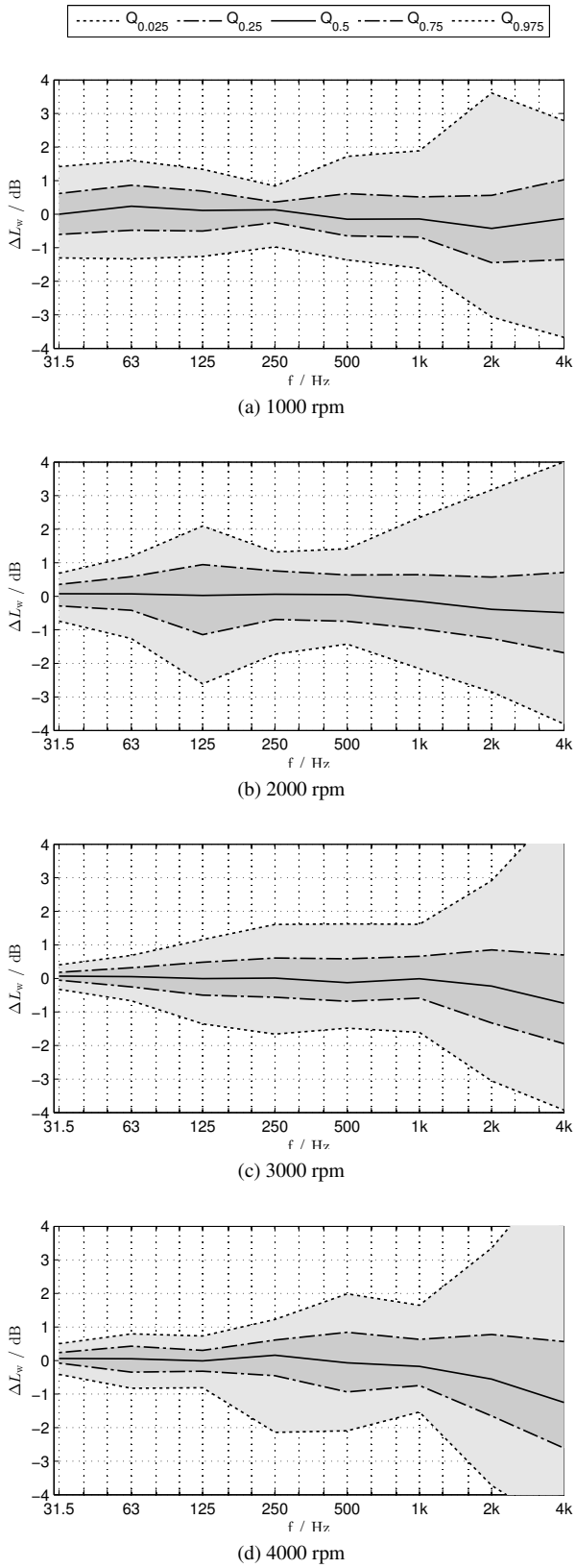

(a) 1000 rpm

(b) 2000 rpm

(c) 3000 rpm

(d) 4000 rpm

Fig. 8: Uncertainty of the tetrahedral grid using the composite near-field-involving estimator, octave band average, (a) 1000 rpm, (b) 2000 rpm, (c) 3000 rpm, (d) 4000 rpm.

field. Comparing the measurement grid proposed in the norm with alternative grids, we discussed desirable measurement grid properties: a) statistical uncertainty is minimized by a uniform spherical sampling grid, b) only then spherical harmonic decomposition is possible, and systematic near field errors can be avoided.

Finally we showed that maximum determinant points combined with a composite near-field-involving sound power estimator achieve the most accurate sound power estimates. This estimate avoids systematic over-estimation errors by taking the minimum of a near-field-involving estimator and the typical squared pressure sum.

ACKNOWLEDGMENT

We thank the Advanced Simulation Technology department of AVL GmbH, Günter Offner and Achim Hepberger, for making available simulated engine data to us. This work was supported by the project ASD, which is funded by Austrian ministries BMVIT, BMWFJ, the Styrian Business Promotion Agency (SFG), and the departments 3 and 14 of the Styrian Government. The Austrian Research Promotion Agency (FFG) conducted the funding under the Competence Centers for Excellent Technologies (COMET, K-Project), a program of the above-mentioned institutions.

REFERENCES

[1] **ISO 3745: Acoustics — Determination of sound power levels and sound energy levels of noise sources using sound pressure — Precision methods for anechoic rooms and hemi-anechoic rooms**, 2012

[2] P. Leopardi: **A partition of the unit sphere into regions of equal area and small diameter**, *Electronic Transactions on Numerical Analysis*, 25(12), 2006, `http://eqsp.sourceforge.net`

[3] R. S. Womersley, I. H. Sloan: **How good can polynomial interpolation on the sphere be?**, *Advances in Computational Mathematics*, 14, 2001, `http://web.maths.unsw.edu.au/~rsw/Sphere/Images/MD/md_data.html`

[4] D. Kirk: **Graphics Gems III**, Academic Press, Inc., 1995

[5] F. Zotter: **Sampling strategies for acoustic holography/holophony on the sphere**, *Fortschritte der Akustik / NAG/DAGA*, Rotterdam, 2007

[6] B. Rafaely, B. Weiss, E. Bachmat: **Spatial aliasing in spherical microphone arrays**, *IEEE Transactions on Signal Processing*, 55(3), 2007